Vibration of submillimeter-size supported droplets

Franck Celestini* and Richard Kofman
Laboratoire de Physique de la Matière Condensée, UMR 6622, CNRS, Université de Nice Sophia-Antipolis, Parc Valrose 06108 Nice Cedex 2, France
(Received 6 September 2005; published 7 April 2006)

We study the fundamental vibration mode of supported submillimeter-size droplets. Using an analogy with a simple oscillator we derive a semianalytical expression for the eigenfrequency and the scaling law of the energy dissipation within the droplet. The experimental results obtained for mercury drops deposited on glass are compared with the model. The agreement is satisfactory for the eigenfrequencies on the whole range of size we considered (from 0.04 to 0.9 mm). The scaling law for the dissipation is recovered for radii larger than 0.1 mm but fails for smaller droplets. We finally discuss possible applications related to the use of vibrations to effectively reduce the hysteresis of the wetting angle and therefore increase the mobility of the supported droplets.

DOI: 10.1103/PhysRevE.73.041602 PACS number(s): 68.08.Bc, 47.55.D−, 68.35.Ja

I. INTRODUCTION

The vibrations of free liquid drops were first investigated more than a century ago by Kelvin [1] and Rayleigh [2]. Later, Lamb [3] found a general expression for the different vibration modes of a free liquid drop surrounded by an outer fluid:

$$\omega_n^2 = \frac{n(n-1)(n+1)(n+2)}{(n+1)\rho + n\rho^f}\frac{\gamma}{R^3}. \quad (1)$$

In this expression, ρ and ρ^f are the densities of the liquid and outer fluid, respectively, n refers to the mode number, and R is the liquid drop radius. The surface tension γ is the driving force for the oscillations and is at the origin of the $-3/2$ exponent in the scaling of frequency with drop size. These pionneering studies have been used and extended in different fields—for example, in the case of nonlinear oscillations of pendant drops [4]. However, the case of a liquid drop in partial contact with a substrate has not been so fully investigated. In the 1980s, microgravity experiments have motivated both experimental and theoretical studies, leading to new results in the case of axisymmetric vibrations [5–7]. Nevertheless, the singularity of the drop shape at the triple line has prevented analytical results. The fundamental mode associated with a longitudinal vibration of the substrate has not been described, and the dependence of the eigenfrequencies on the wetting angle has never been fully examined.

If it is well known [8] that vibrations can help in probing the energy barriers responsible for the wetting angle hysteresis, the effect of vibrations on the mobility of supported drops has just been recently demonstrated [9,10]. These new studies are motivated by numerous applications in microfluidics [11] and microelectronics [12]. They could also be of importance in understanding fundamental questions associated with the contact line motion. The driving force for the drop mobility can be achieved in different ways—for example, with substrates with surface tension gradient [13–15] or using the electrowetting effect [16]. Nevertheless, in both cases the drop mobility is reduced because of the wetting angle hysteresis [17]. The main idea is therefore to use vibrations of the substrate or another oscillating external force acting on the drop in order to effectively reduce the hysteresis. Promising results have been obtained very recently [18], and possible applications are currently under study.

The aim of this paper is to fully characterize the fundamental vibration mode of a supported drop. It is associated with vibrations of the substrate parallel to the surface. This mode is the one that should have the most important influence on the drop mobility because the vibrations induce an increase and a decrease of the advancing and receding wetting angles, respectively (Fig. 1). For a sufficiently large vibration we expect to reach the wetting angle hysteresis threshold and, under the influence of an external force, eventually move the droplet. We will not consider the second mode corresponding to perpendicular vibrations of the substrate but a similar approach to the one presented in this paper can also be used for its characterization. An analogy with a simple oscillator will be presented in the model section from which we will propose a semianalytical expression for the eigenfrequency and a scaling law of the dissipation term with drop size. We will present the chosen system and the measurement techniques in the experimental section (Sec. III). The experimental results obtained for a mercury drop deposited on glass will be compared to the model in

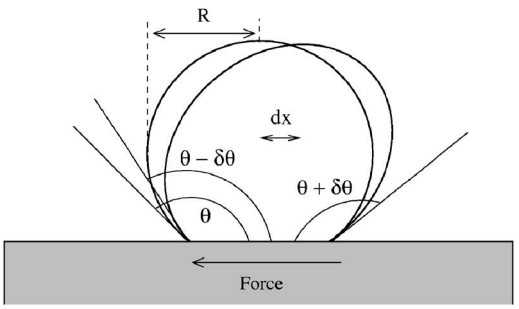

FIG. 1. Schematic representation of the droplet shape under the influence of an external force. The deformation induces a displacement dx of the center of mass and a variation $\delta\theta$ of the advancing and receding wetting angles.

*Electronic address: Franck.Celestini@unice.fr

Sec. IV. We will finally discuss our results and some prospects in the Conclusion.

II. MODEL

We first concentrate on the eigenfrequency ω_0 of a supported droplet vibrated in a direction parallel to the substrate. For a sufficiently weak external force the triple line remains fixed and the surface is deformed. The deformation is characterized by the displacement dx of the center of mass and by the variation $\delta\theta$ of the advancing and receding wetting angles θ_a and θ_d (Fig. 1). We call θ the equilibrium wetting angle and assume a symmetric variation of the wetting angles: $\theta_a=\theta+\delta\theta$ and $\theta_r=\theta-\delta\theta$. We note $\Delta S=S-S_0$, the surface variation associated with the deformation where S_0 is the surface of the droplet at equilibrium and S its surface under the influence of an external force. We can write ΔS as

$$\Delta S = S_0 f(\theta)\delta\theta^2, \tag{2}$$

where we include the linear relations between ΔS and S_0 and between ΔS and $\delta\theta^2$. The function $f(\theta)$ takes into account the fact that the precise relation between these quantities depends on the equilibrium wetting angle value. The limiting case where θ tends to π helps understand the role of $f(\theta)$. In this case the droplet has a small contact area with the substrate; for $\theta=\pi$, the contact reduces to a point and the droplet can freely rotate around it without any deformation. The limit value of $f(\theta)$ when θ tends to π is therefore 0. One can easily see that this is no longer the case when $\theta<\pi$. We can also write, for the displacement of the center of mass,

$$dx = g(\theta)R\delta\theta. \tag{3}$$

In this expression R is the radius of the truncated sphere (Fig. 1) and $g(\theta)$ a second function depending on the system geometry.

Combining the two previous expressions we obtain

$$\Delta S = \frac{S_0 h(\theta)}{R^2} dx^2, \tag{4}$$

where $h(\theta)=f(\theta)/g(\theta)^2$. A restoring force $F=-\gamma\Delta S/dx$ is associated with the deformation. It reads

$$F = -\frac{\gamma S_0 h(\theta)}{R^2} dx, \tag{5}$$

where γ is the surface tension between the liquid and vapor. The restoring force is linear in the displacement of the center of mass so that we can define an effective spring constant k_e and the eigenfrequency of the droplet, $\omega_0=\sqrt{k_e/\rho V}$. Using the expressions for the surface S_0 and the volume V of a truncated sphere we finally write

$$\omega_0 = \sqrt{\frac{6\gamma h(\theta)}{\rho(1-\cos\theta)(2+\cos\theta)}} R^{-3/2}, \tag{6}$$

where ρ is the liquid density. In this expression the dependence on the geometry is included on $h(\theta)$. We compute $h(\theta)$ under the hypothesis that the deformation is the one obtained at equilibrium—i.e., that the deformation is the one that minimizes the free energy of the droplet under the influence of a constant external force. This hypothesis can be checked looking at the capillary number $C_a=\eta V/\gamma$ that measures the relative importance of viscous and capillary pressures. For the system considered experimentally the values of C_a are well below unity, justifying the assumption of an equilibrium deformation due to the predominance of capillary effects.

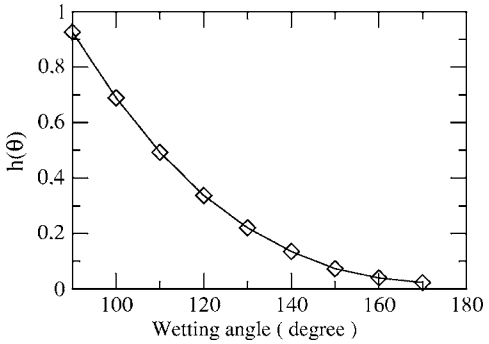

FIG. 2. Numerical values obtained for $h(\theta)$.

We use the program surface evolver (SE) [19] to numerically compute the function $h(\theta)$. We first simulate a drop wetting a substrate parallel to the (Ox,Oz) plane. The wetting angle is given as an input parameter, and we fix the triple-line position. We therefore use the gravity constant of the SE to apply an external force to the droplet. Under the influence of this external force, parallel to the substrate and applied to the overall droplet volume, the drop reaches the equilibrium shape that minimizes its free energy. For different values of the gravity constant we record the different quantities we are interested in: the advancing and receding wetting angles θ_a and θ_r, the position of the center of mass dx, the surface variation ΔS, and the ghost radius variation dR, which will be discussed and used in the experimental section. For what concerns the numerical estimate of $h(\theta)$, we first plot ΔS versus dx to verify the expected quadratic relation. Since S_0 and R are known quantities, a best fit to Eq. (4) permits us to obtain $h(\theta)$. The same procedure is used for different values of the wetting angle. Calculated values of $h(\theta)$ for wetting angles ranging between 90° and 170° are represented in Fig. 2. Note that we recover the limiting case discussed above for which $h(\theta)$ tends to zero when θ tends to π. This function is not material dependent and could therefore be used in the future for different systems. It should also permit one, for example, to determine the angle of a tilted plane above which the gravity force becomes larger than the sticking one due the wetting angle hysteresis [20]. More generally this function permits one to obtain the characteristic capillary time of a supported droplet as a function of its wetting angle.

In the experiments presented below an inertial force is applied to the droplet through the vibration of the substrate. The substrate momentum diffuses within the liquid over a distance $\delta=\sqrt{2\mu/\omega}$ known as the Stokes length where μ is the kinematic viscosity. Above this distance the droplet therefore experiences the inertial force. This situation is different of the simulated one using the SE. Indeed in the numerical analysis the external force is applied to the overall

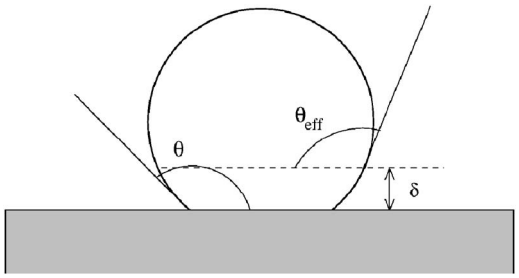

FIG. 3. Schematic representation of the effective wetting angle associated with the Stoke length.

droplet volume. A first-order correction consists in defining an effective equilibrium wetting angle θ_{eff} (Fig. 3). In the limit of a small Stokes length as compared to the droplet radius $\left(\frac{\delta}{R\sin\theta} \ll 1\right)$ we have

$$\theta_{eff} = \theta - \frac{\delta}{R\sin\theta}. \tag{7}$$

Finally, the corrected eigenfrequency can be calculated using Eq. (6) but replacing the true equilibrium wetting angle θ by the effective wetting angle value θ_{eff}.

In the limit of weak vibrations the position of the droplet center of mass (in the vibrating frame) satisfies the differential equation

$$\ddot{x} + \alpha\dot{x} + \omega_0^2 x = a_0\cos(\omega t), \tag{8}$$

where a_0 is the acceleration due to the substrate vibration and ω_0 the eigenfrequency discussed just above. We now need to identify the dissipation term α to fully characterize the oscillating drop. Since we here describe the regime with a fixed triple line, the dissipation is due to the diffusion of the substrate momentum within the liquid and therefore to the associated shear stress. This occurs on a distance of the order of the Stokes length δ. The associated viscous force F_s therefore scales as

$$F_s \propto \frac{S_c\eta}{\delta}\dot{x}, \tag{9}$$

where S_c is the contact area with the substrate and η the liquid viscosity. Since $\alpha \propto F_s R^{-3}$, $S_c \propto R^2$, and $\delta \propto \omega^{-1/2}$ with $\omega = \omega_0 \propto R^{-3/2}$ at the resonance, we therefore expect the scaling

$$\alpha \propto R^{-7/4} \quad \text{and} \quad Q \propto R^{1/4}, \tag{10}$$

respectively, for the inverse of the characteristic dissipation time α and $Q = \omega_0/\alpha$ the quality factor of the oscillating droplet. It is important to note the weak size dependence of Q, meaning that the resonance effect should be present even for very small droplets.

III. EXPERIMENT

We choose to study mercury drops deposited on glass slides. The liquid drop has a wetting angle of 140°. The glass slides are first cleaned with a detergent after what they are put into a freshly prepared piranha solution (30% H_2O_2 and 70% H_2SO_4) for 20 min. They are finally rinsed with an ultradistilled water and dried under pure nitrogen. Mercury drops with radius ranging roughly between 0.05 and 1 mm have been studied. For the larger drops a microsyringe is used for the deposition while the smallest ones are producted using a thin capilar tube with an outer diameter of 70 μm. Once the drop is deposited, the glass slide is inserted in the vibrating apparatus presented in Fig. 4. A nitrogen flow is necessary to prevent the oxidation of mercury. A low-frequency signal is sent to the vibrator through an amplificator, and the oscillation amplitudes of the plate are optically measured with a photodiode. A video camera is used to visualize the drop, and the image is formed through a mirror attached to the vibrating plate. We therefore just visualize the vibration induced to the drop by the substrate. The time exposure of the camera being larger than the applied vibration period we record ghost images of the drop. This is illustrated in Fig. 5 for a drop with radius 0.192 mm vibrated at a frequency of 252 Hz.

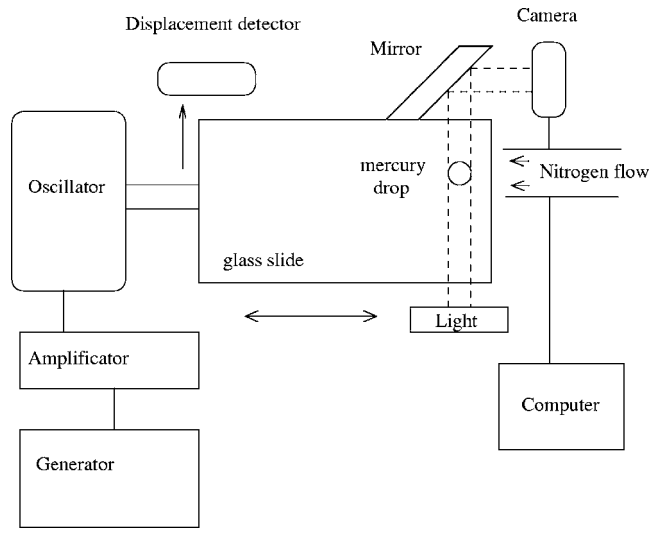

FIG. 4. Schematic representation of the experimental apparatus.

In the same manner that we found the relation between the surface variation and the center-of-mass displacement,

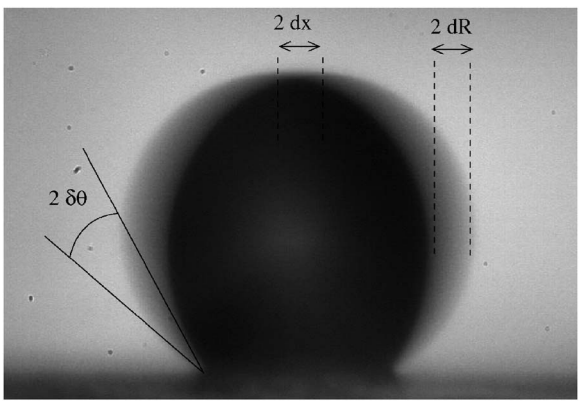

FIG. 5. Image of a vibrating $R = 0.192$ mm mercury drop. The measure of the ghost radius variation dR permits to calculate both $\delta\theta$ and dx.

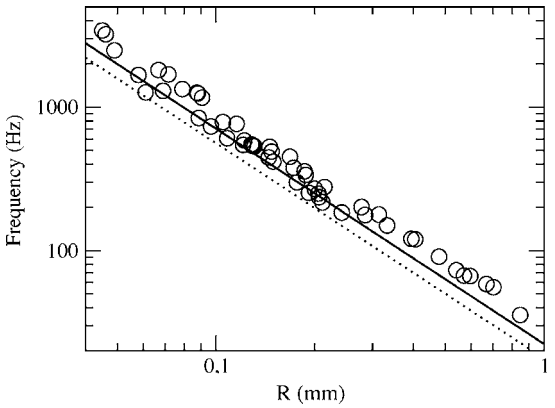

FIG. 6. Eigenfrequency as a function of the drop size. The dotted and solid lines are calculated using Eq. (6), respectively, with $\theta=140°$ and $\theta=\theta_{eff}=130°$.

we use the SE to obtain the relation between the ghost radius variation dR and the associated wetting angle variation $\delta\theta$ (Fig. 5). For a wetting equilibrium angle of 140° we found $\delta\theta \simeq 96.5 dR/R°$. To fully and quantitatively describe the drop oscillations we also need the relation between $\delta\theta$ and the associated displacement of the center of mass dx (Fig. 5) as expressed in Eq. (3). Once again we use the SE to numerically evaluate $g(\theta=140°)$ and obtain the relation $\delta\theta=102.7\, dx/R$.

IV. RESULTS

We first concentrate on the eigenfrequency of the drops. A simple manner to determine it is to find the frequency for which dR is maximum. This is what we do for mercury drops with radius ranging between roughly 0.04 and 0.9 mm. We present in Fig. 6 the eigenfrequency as a function of the drop size. The dotted line corresponds to Eq. (6) with a value of $\theta=140°$ corresponding to the true wetting angle of mercury on glass. We can see that the $-3/2$ exponent is recovered but that the model seems to underestimate the eigenfrequency value. We therefore use the correction to θ due to the Stokes length [Eq. (7)]. For the drop size considered in this study the correction is roughly 10°. The full line in Fig. 6 therefore represents Eq. (6) with $\theta=\theta_{eff}=130°$. Even if the agreement is better, we still underestimate the eigenfrequency. This means that the correction has to fully take into account the deformation within the region near the substrate. Nevertheless, the model gives a reasonable prediction (the underestimation is roughly 15%) without any adjustable parameter. A similar agreement has been found looking at the eigenfrequency of the second mode, corresponding to a vibration perpendicular to the substrate. The same approach has been used to obtain a semianalytical expression, and the results will be presented elsewhere [21]. We also verified that the model gives a good agreement with the experimental data recently obtained [10,18] for water droplets.

We now turn to the characterization of the energy dissipation. The resonance effect can be illustrated by measuring the amplitude of the wetting angle variation as a function of the applied frequency f. This can be achieved for different values of the substrate acceleration. We represent, in Fig. 7, $\delta\theta$ as a function of f for the two accelerations $a_0=0.48$ and

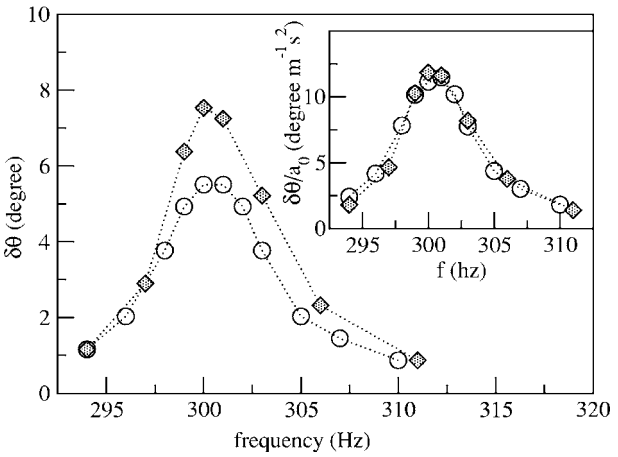

FIG. 7. Amplitude of the wetting angle variation $\delta\theta$ as a function of the frequency vibration. The circles and diamonds, respectively, correspond to substrate accelerations $a_0=0.48$ and 0.63 ms^{-2}. In the inset $\delta\theta$ is normalized by a_0 to verify the linear response of the drop oscillator.

0.63 ms^{-2} and for a droplet of radius $R=0.176$ mm. As expected $\delta\theta$ passes through a maximum at the eigenfrequency f_0 and we recover a typical resonance plot. It is also not surprising to see that the larger the substrate accelerations, the larger the $\delta\theta$ values get. In the inset we represent the same quantity but normalized by the substrate acceleration. In this case the two data sets lie on the same curve. This means that, for the acceleration considered here, the response of the oscillator is linear and that the hypothesis of a fixed triple line is valid. One could extract from this curve the bandwidth $\Delta f=\alpha/4\pi$ and therefore characterize the energy dissipation. For example, from Fig. 7 we found $\Delta f \simeq 6$ Hz for the considered droplet. Nevertheless, the procedure is rather complicated because we have to measure several resonance curves in order to verify the linear response of the system. We therefore choose a different procedure to characterize the dissipation. It consists, for different fixed substrate accelerations, of measuring the maximum wetting angle variation—i.e., to measure $\delta\theta$ at the eigenfrequency ω_0. For the simple oscillator considered here, we know that, at the resonance, $dx=a_0/\omega_0\alpha$. Using the relation between dx and $\delta\theta$ given in the experimental section we expect a linear relation $\delta\theta=pa_0$. A measure of the slope p therefore permits us to extract the value of α and the associated bandwidth Δf:

$$\Delta f = \frac{96.5}{4\pi\omega_0 R p}. \tag{11}$$

We represent, in Fig. 8, $\delta\theta$ as a function of a_0 for two droplets with radius 0.177 and 0.149 mm. We recover a linear relation for the weaker accelerations which confirms the observation from the inset of Fig. 7. For larger a_0 values, the curve deviates from linearity and tends to saturate. We interpret this behavior in the following manner: when $\delta\theta$ reaches the value of the wetting angle hysteresis, the triple line starts to move and part of the substrate acceleration is used for this motion. As a consequence the angle amplitude variation saturates. The same qualitative behavior is observed for the two

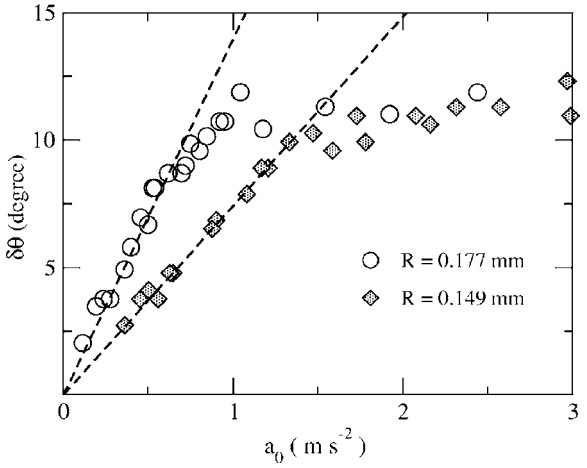

FIG. 8. Maximum wetting angle variation $\delta\theta$ as a function of the substrate acceleration for two droplets with R=0.177 and 0.149 mm.

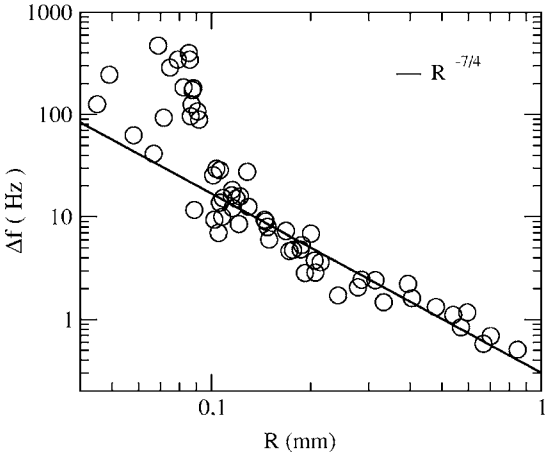

FIG. 9. Inverse of the relaxation time α as a function of the droplet radius. The solid line represents the best fit to the expected scaling law [Eq. (9)] for the larger droplet sizes.

particles. More quantitatively, we can remark that the value of $\delta\theta$ at which we reach saturation is the same for the two droplets and roughly equal to 10°. As stressed just above this gives us an estimate of the wetting angle hysteresis which, as expected, is not size dependent. A similar transition from a pinned to a mobile triple line has been recently observed for a sessile drop of water [22]. In this work the large-radius droplets permit us to directly measure both the triple-line position and the droplet deformation. This is not possible in our case, and we detect the contact-line motion through the nonlinearity of the $\delta\theta$ versus a_0 curve. Another way of detecting the contact-line motion is to look at the frequency at which $\delta\theta$ is found to be maximum for different substrate accelerations. In the linear regime the eigenfrequency is a constant as expected for an oscillator with a constant dissipation factor. Conversely, when we reach the nonlinear regime, the contact-line motion induces a supplementary dissipation source that lowers the eigenfrequency.

In the linear regime the slope is higher for the larger droplet. Since p is inversely proportional to α, we recover here the prediction of a larger dissipation for the smaller droplets. To quantitatively test the scaling law given by Eq. (10) we measure Δf for different droplet sizes. We plot, in Fig. 9, Δf as a function of R in a log-log representation. We first verify that we obtain values of Δf that are in good agreement with the ones directly obtained from the $\delta\theta$ versus f plot (Fig. 7). The solid line represents the best fit to the expected scaling law for the larger droplet sizes. The agreement between the model and experiment is satisfactory for drops with radius roughly above 0.1 mm. Conversely, below this size the dissipation is found to be much larger than expected. We performed a lot of measurements in this region to confirm this apparent crossover and found that the dispersion in the experimental data increases as the droplet size decreases. We have also verified that the disagreement is not due to the way we prepare and deposit the drop on the substrate. It is important to note that for the same drop the scaling law for the eigenfrequency is respected while we found a large disagreement for the dissipation term. Since the eigenfrequency is governed by the liquid-vapor interface deformation, it is therefore reasonable to think that a phenomenon is occurring at the contact area between the liquid and substrate. The most probable explanation is that for the lower sizes the hypothesis of a fixed triple line is no longer valid. We therefore think that the substrate acceleration induces both a surface deformation and a triple-line motion. At present we cannot definitely explain why such a behavior is obtained for the smallest droplet sizes and plan to perform a similar experiment on different substrates.The crossover could be due to the presence of impurities on the surface but also to the onset of slip at the liquid-solid interface.

V. CONCLUSIONS AND PERSPECTIVES

To summarize, we have used an analogy with a simple oscillator to extract a semianalytical expression for the eigenfrequency of a supported droplet and a scaling law for the energy dissipation. We concentrate here on the fundamental vibration mode corresponding to a parallel vibration of the substrate (rocking mode). The agreement found between the model and experiment is rather good for the eigenfrequency without any free parameter. The expression given by Eq. (6) together with the numerical values of $h(\theta)$ (Fig. 2) could therefore be used in the future to obtain a reasonable prediction of the eigenfrequency whatever system (i.e., the wetting angle) considered.

If the scaling law for the dissipation is verified for the largest considered droplets, a large discrepancy is found for a radius roughly below 0.1 mm. We cannot give a definite explanation for this crossover. We nevertheless think that it is related to the fact that for such drops substrate accelerations, even weak, induce both a drop deformation and a contact-line motion. This behavior is qualitatively different from the one predicted and verified for the larger droplets. In this case, for the weaker accelerations the drop is simply deformed with a fixed triple line. Its motion appears when the amplitude of the wetting angle variations is larger than the hysteresis. We plan future experiments to understand why this scenario is not recovered for smaller droplets.

[1] Lord Kelvin, Mathematical and Physical Papers **3**, 384 (1890).
[2] Lord Rayleigh, *The Theory of Sound* (Macmillan, New York, 1894).
[3] H. Lamb, *Hydrodynamics* (Cambridge University Press, Cambridge, England, 1932).
[4] O. A. Basaran and D. W. DePaoli, Phys. Fluids **6**, 2923 (1994).
[5] M. Strani and F. Sabetta, J. Fluid Mech. **141**, 233 (1984).
[6] R. W. Smithwick and J. A. M. Boulet, J. Colloid Interface Sci. **130**, 588 (1988).
[7] H. Rodot, C. Bisch, and A. Lasek, Acta Astron. **6**, 1083 (1979).
[8] E. L. Decker and S. Garoff, Langmuir **12**, 2100 (1996).
[9] S. Daniel and M. K. Chaudhury, Langmuir **18**, 3404 (2002).
[10] S. Daniel, S. Sircar, J. Gliem, and M. K. Chaudhury, Langmuir **20**, 4085 (2004).
[11] M. G. Pollack, R. B. Fair, and A. D. Shenderov, Appl. Phys. Lett. **77**, 1725 (2000).
[12] J. Simon, S. Saffer, and C. J. Kim, J. Microelectromech. Syst. **6**, 208 (1997).
[13] H. P. Greenspan, J. Fluid Mech. **84**, 125 (1978).
[14] F. Brochard, Langmuir **5**, 432 (1989).
[15] T. Ondarcuhu and M. Veyssie, J. Phys. II **1**, 75 (1991).
[16] G. Beni and S. Hackwood, Appl. Phys. Lett. **38**, 207 (1981).
[17] P. G. de Gennes, Rev. Mod. Phys. **57**, 827 (1985).
[18] S. Daniel, M. K. Chaudhury, and P. G. de Gennes, Langmuir **21**, 4240 (2005).
[19] See K. A. Brakke, http://www.susqu.edu/facstaff/b/brakke/evolver
[20] D. Quéré, Langmuir **14**, 2213 (1998).
[21] F. Celestini and R. Kofman (unpublished).
[22] X. Noblin, A. Buguin, and F. Brochard-Wyart, Eur. Phys. J. E **14**, 395 (2005).